Desalination and Water Treatment
www.deswater.com

doi: 10.5004/dwt.2022.28809

271 (2022) 206–219
September

Utilization of palm leaves as an extraordinary adsorbent for the removal of Pb(II) from an aqueous solution

Ismail W. Almanassra†, Muhammad Imran Khan*,†, Anjaneyulu Chatla†, Muataz Ali Atieh*, Abdallah Shanableh*

Research Institute of Sciences and Engineering, University of Sharjah, Sharjah 27272, United Arab Emirates, emails: raoimranishaq@gmail.com/mimran@sharjah.ac.ae (M.I. Khan), mhussien@sharjah.ac.ae (M. Ali Atieh), shanableh@sharjah.ac.ae (A. Shanableh), ialmanassra@sharjah.ac.ae (I.W. Almanassra), achatla@sharjah.ac.ae (A. Chatla)

Received 16 March 2022; Accepted 3 August 2022

ABSTRACT

Heavy metal such as lead (Pb(II)) is non-biodegradable and bio accumulative that posture a threat to our health when it presents in huge amount in our bloodstream. It comes from mostly chemical industrial processes into wastewater. In this study, we reported the adsorption of Pb(II) onto palm leaves from an aqueous solutions. The characterization results illustrated that the palm leaves have a mesoporous structure with a pore volume of 0.017 cm^3/g. The successful removal of Pb(II) ions by palm leaves was confirmed by using Fourier transform infrared and scanning electron microscopy analysis. The influence of contact time, mass of palm leaves, initial concentration of Pb(II) in aqueous solution, temperature and pH on the removal of Pb(II) was explored. Kinetic study represented that Pb(II) adsorption fitted to pseudo-second-order model with a correlation factor (R^2) of 1. The equilibrium outcomes showed that the experimental data followed to Langmuir isotherm with an R^2 of 0.990 and a maximum adsorption capacity of 57.4 mg/g. Adsorption thermodynamics investigation showed that Pb(II) adsorption onto palm leaves was an endothermic, feasible and spontaneous. The palm leaves demonstrated a removal efficiency of more than 59% of Pb(II) after 5 consecutive adsorption/desorption cycles. Hence, the palm leaves could be employed as an excellent candidate for Pb(II) adsorption from aqueous solutions.

Keywords: Langmuir isotherm; Adsorption; Pb(II); Endothermic process; Palm leaves

1. Introduction

Lead is one of the most toxic metal among heavy metals for the human health especially for children because of the fact that, their growing bodies can absorb higher quantities of Pb(II) than adults [1–3]. It has fuels applications in explosive manufacturing, printing, pigments manufacturing, and photographic materials [4]. Although Pb(II) is forbidden in several products, it is still employed in commercial products as automotive batteries, cookware, paints, and some Mexican potter glazes [5,6]. Some not dangerous diseases including anemia, diarrhea, and headaches are seen at a low concentrations of Pb(II) ions in the blood, while, at a higher concentration (>10 μg/L), the liver, kidney, and neurological and reproductive systems can be seriously damaged [7,8]. Hence, the small concentration of Pb(II) is also very toxic for living organism and human being [9,10].

The aquatic ecosystem has been continuously influenced by the direct and indirect removal of industrial wastes worldwide, possessing several organic and inorganic

* Corresponding author.
† Authors contributed equally to this work.

pollutants with the industrial revolution and social development of human activities [11]. Pb(II) is employed on a large scale in many industrial processes and have achieved reasonable attention receivable to their toxicity to living organisms and non-biodegradability [12]. Further, it is a worldwide contaminant because of its many life-terrifying effects, namely brain disorders in children. Substantially, Pb(II) salts and organic Pb(II) compounds are most dangerous ecotoxicologically. P(II) at pH < 6 is a well-known water pollutant even at very low concentrations it is highly toxic, receiving to its bioaccumulation characterizations, making it harmful to the environment. P(II) species concentration extraordinary declined over pH 6 because of the formation of $Pb(OH)^+$, $Pb_3(OH)_4^{3-}$ and $Pb(OH)^2(aq)$ precipitates [13]. According to the US Environmental Protection Agency, the maximum bearable limit for Pb(II) in drinking water is 0.05 mg/L [14]. The report of the Institute for Health Metrics and Evaluation showed that yearly deaths of more than half a million worldwide are due to the exposure of Pb(II). Moreover, anthropogenic activities repeatedly result Pb(II) pollution in the environment, particularly through wastewater removal [15]. Hence, suitable materials must be designed to remove Pb(II) from an aqueous solution.

To date many procedures including ion exchange [16], chemical precipitation [17], coagulation [18], floatation [19], membrane processes [20], solvent extraction [21] and adsorption [22,23] were utilized to remove heavy metals from an aqueous solutions. Adsorption as the mostly employed procedure among them to remove heavy metals due to its significance over other reported methods which are easy operation, low cost, production of less sludge volume and high efficiency [24–27]. Adsorbents can be classified into various groups such as zeolites, chemical adsorbents, and nano-adsorbents, bio adsorbents [28]. A wide range of adsorbents were used to remove Pb(II) ions from an aqueous solutions including zeolites, carbon based materials, modified nanomaterials and bio sorbents [29–31]. However, in the last two decades, the utilization of agricultural wastes in elimination of contaminants and emerging pollutants is exponentially growing. The date palm tree considered one of the oldest basic crops in UAE. More than 40 million palm trees are available in UAE which makes UAE one of the top ten producers of palm in the world. Around 15 to 20 kg of agriculture waste is produced annually from each palm tree and most of these wastes are transferred out of the farms which are considered additional cost on the farmers. These wastes including the different parts of the tree including branches, fronds, leaves, stem barks and rachis. Hence, this great amount of wastes can be utilized in environmental applications which in turn contribute toward a sustainable system. The palm tree leaves in Algeria and Iran were utilized for Pb(II) removal and the results demonstrated a promising material for the remediation of Pb(II) ions from water. However, these studies didn't cover the application of various adsorption isotherm and kinetic models. Moreover, different kinds of palm trees are globally available. The type of palm trees is not mentioned in these studies; in our case we have used Phoenix sylvestris generation, a well-known and widely cultivated palm tree in UAE. Herein, we utilized Phoenix sylvestris palm leaves as adsorbent for the removal of Pb(II) from aqueous solutions. The adsorptive removal of Pb(II) from aqueous solutions onto Phoenix sylvestris palm leaves was not reported to the best of our knowledge yet.

In this manuscript, batch adsorption of Pb(II) from aqueous solutions onto palm leaves was reported. The effect of contact time, mass of adsorbent, initial concentration of Pb(II) in aqueous solution, temperature and pH on the removal of Pb(II) was investigated. FRIR spectroscopy was utilized to prove adsorption of Pb(II) onto palm leaves. Morphology of palm leaves was studied by using scanning electron microscopy (SEM). For Pb(II) adsorption onto palm leaves, kinetics, isotherms, and thermodynamics were also revealed. Moreover, the reusability of the palm leaves toward Pb(II) ions removal was evaluated by conducting a series of adsorption/desorption experiments.

2. Experimental

2.1. Materials

Lead nitrate $Pb(NO_3)_2$ (purity ≥ 98%), sodium hydroxide (NaOH, purity ≥ 98%), hydrochloric acid (HCl, purity 37%) were kindly supplied by Sinopharm Chemical Reagent Co., Ltd., Shanghai, China. All the chemicals were utilized as received. Throughout this work, deionized water was utilized.

2.2. Adsorbent

The biomass feed (palm leaves) was obtained from local palm trees available in the sustainability garden of the University of Sharjah, Sharjah, United Arab Emirates. The palm tree leaves were washed with deionized water to remove dust particles and debris. The leaves were then cut into small pieces as seen in Fig. 1 and oven dried at 80°C over a 24 h to evaporate water. Finally, the palm leaves were grinded at a size of <0.25 mm using ultra centrifugal mill (model ZM 200, Retsch, Germany). Fig. 1 illustrates a general schematic of palm leaves powder preparation.

2.3. Batch adsorption of Pb(II) onto palm leaves

Adsorption of Pb(II) ions onto palm leaves was performed as described in our previous research [25–27,32–35].

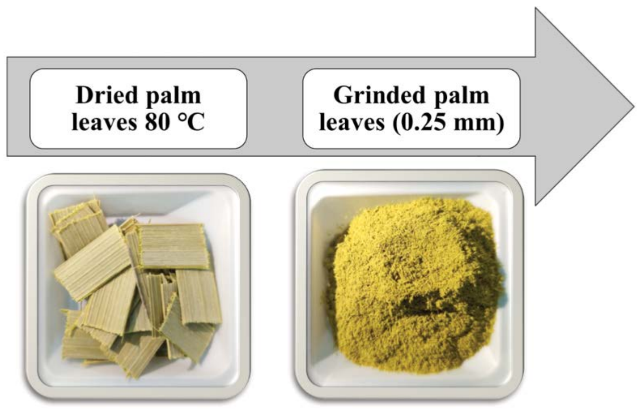

Fig. 1. General schematic of palm leaves preparation.

Briefly, a determined quantity of palm leaves was taken into a 25 cm^3 secured cap culture tube along with 4 cm^3 of standard acid solution and a constant volume of stock radiotracer with measured mass of Pb(II) ions concentration solution was added. Consecutively, the contents were equilibrated on a wrist-action mechanical shaker (Vibromatic, USA) at a rate of 200 RPM for specific intervals of time. Then, it was centrifuged at 5,000 rpm for phase separation and the supernatant solution was withdrawn for activity measurement. The radioactivity of solutions before (A_i) and after (A_f) equilibrium was calculated with a NaI well type scintillation counter (Canberra Inc.) coupled with a counter-scaler (Nuclear Chicago). A volume of 1.0 cm^3 was normally used to record activity. All research was recorded at room temperature. Each experiment repeated three times and average values were presented throughout the manuscript. The percentage removal of Pb(II) was determined using below relationship:

$$\% \text{ adsorption} = \frac{A_i - A_f}{A_i} \times 100 \quad (1)$$

where A_i and A_f indicate initial and final adsorption of Pb(II) (counts/min) into an aqueous solution respectively. Table 1 provides the detailed experimental conditions of the current study.

2.4. Reusability studies

In the regeneration studies, the adsorption experiment was carried out by shaking 200 mL of 30 mg/L of Pb(II) and 600 mg of palm leaves (i.e., adsorbent dose of 3 g/L). Then Pb(II) loaded palm leaves were separated from the solution by centrifugation and then washed with 200 mL of 0.1 M HCl. Desorption experiments were agitated at room temperature using agitation speed of 250 RPM, for 5 h. After that, the acid treated palm leaves were washed with DI until neutral pH was achieved and then, the same palm leaves were used in the next adsorption experiments. This procedure was followed 5 times.

2.5. Characterization

The Brunner–Emmett–Teller (BET) surface area, pore size distribution and pore volume were investigated by the nitrogen adsorption/desorption experimentation using the NOVATECH LX2 analyzer, Anton Paar, Austria. The equipment was degassed at 300°C for 6 h before conducting the test. Palm leaves were studied before and after Pb(II) adsorption by using Fourier transform infrared (FTIR spectrometer, Vector 22, Bruker, Germany) containing resolution of 2 cm^{-1} and total spectral range of 4,000–400 cm^{-1} with attenuated total reflectance. Field emission scanning electron microscope (FE-SEM, Sirion200, FEI Company, USA) was utilized for investigating morphological features of palm leaves. The SEM is equipped with energy dispersive spectroscopy (EDS, Bruker Xflash 6/60, Germany) used for elemental analysis. The zero point of charge (pH_{PZC}) was evaluated by the pH drift method [36]. Briefly, 20 mg of palm leaves powder was added to 6 containers containing 20 mL of 0.1 M NaCl. The pH of each container was adjusted between pH 2 and 12 using 0.1 M of NaCl and 0.1 M of HCl. The container was allowed to shake at room temperature using agitation speed of 200 RPM for 72 h. The final pH was measured and the PZC was evaluated. The crystallinity of the palm leaves before and after adsorption was evaluated by X-ray diffraction (XRD, D8 Advance, Bruker, Germany) using a wave length of 1.5 Å and angle range of 2θ between 10° and 80°.

2.6. Adsorption kinetics

The adsorption kinetic data were investigated by different kinetic models including pseudo-first-order, pseudo-second-order, Elovich, liquid film diffusion, modified Freundlich equation and Bangham models. These models were compared to each other by testing the kinetic data on the linearized models. The comparison was made based on the value of the correlation factor (R^2). The kinetic model equations, linearized forms and their parameter are presented in (Section S1 for detail in supporting information).

Table 1
Detailed experimental parameters and conditions

Parameters	Investigated range	Other experimental conditions
Influence of palm leaves dosage	0.01–0.06 g	Initial Pb(II) concentration: 30 mg/L, temperature: 22°C, contact time 1,440 min, initial solution pH 4.8
Influence of contact time	1–1440 min	Initial Pb(II) concentration: 30 mg/L, temperature: 22°C, initial solution pH 4.8, palm leaves dosage 0.03 g
Influence of initial solution pH	2.8–7.4	Initial Pb(II) concentration: 30 mg/L, temperature: 22°C, contact time 1,440 min, palm leaves dosage 0.03 g
Influence of temperature	22°C–55°C	Initial Pb(II) concentration: 30 mg/L, contact time 1440 min, initial solution pH 4.8, palm leaves dosage 0.03 g
Influence of initial Pb(II) concentration	30–500 mg/L	Temperature 22°C, contact time 1,440 min, palm leaves dosage 0.03 g, initial solution pH 4.8
Agitation speed	–	200 rpm for all of the experiments
Sample volume	–	20 mL for all of the experiments

2.7. Adsorption isotherms

Isotherm studies are usually investigated to provide an idea about the interaction between the adsorbent and the adsorbate, moreover, isotherms can predict the maximum adsorption capacity. The isotherm data were subjected to four isotherm models Langmuir, Freundlich, Temkin and Dubinin–Radushkevich. The isotherm data were tested based on the linearized forms of the models. Models were compared to each other according to the R^2 values. Isotherm models, linearized forms and parameters details are provided in (Section S2 for detail in supporting information).

2.8. Thermodynamics study

The values change in Gibb's free energy ($\Delta G°$), enthalpy ($\Delta H°$) and entropy ($\Delta S°$) were measured to study adsorption thermodynamics for Pb(II) as described [25,37] (Section S3 for detail in supporting information).

3. Results and discussion

3.1. Characterization

3.1.1. Textural properties

The surface area of the palm leaves was investigated by the BET method while the porosity properties and pore size distribution were examined by Barrett, Joyner, and Halenda (BJH) method. The palm leaves found to demonstrate a surface area of 3.6 m²/g. Fig. 2 illustrates the N_2 adsorption/desorption isotherm of palm leaves. The N_2 isotherm curve is similar to type IV sorption isotherm implying a mesoporous material according to IUPAC classification. The average pore diameter found to be 14.7 nm. According to the BJH analysis, the pore volume of palm leaves particles was 0.017 cm³/g.

3.1.2. SEM, EDS, XRD and FTIR analysis of palm leaves before and after Pb(II) adsorption

SEM-EDS analysis was carried out on palm leaves adsorbent before and after Pb(II) adsorption and the corresponding images displayed in Figs. 3 and 4. It can be seen that the palm leaves showed irregular shaped particles and it contained different elements such carbon (59.2 wt.%), oxygen (35.4 wt.%), silicon (4.3 wt.%), and some other elements with minute portion. While, after Pb(II) adsorption the palm leaves adsorbent structure was slightly changed which could be the particles segregation during adsorption and elements such as carbon (57.4%), oxygen (31.5%), silicon (4.4%) and Pb (5.7%) and further EDS composition confirmed the successful Pb(II) adsorption onto the palm leave.

FTIR analysis of palm leaves before and after Pb(II) adsorption was conducted to investigate the role of functional groups on the Pb(II) removal adsorption process and the acquired results presented in Fig. 5. Fig. 5a shows the FT-IR spectra recorded in the range of 4,000–400 cm⁻¹ from fresh and spent palm leaves. The fresh palm leaves showed a broad peak around 3,339 cm⁻¹ is assigned to the O–H stretching vibration of carboxylic acid alcohol and phenol groups of palm leaves [38]. The peak at 2,941 and 2,847 cm⁻¹ are attributed to alky (–CH) and C=O stretching vibration [39] and also the peak at 1,738 cm⁻¹ is related to C–O of carboxyl, aldehyde, ketone, and ester groups. The peak around 1,630 cm⁻¹ is ascribed to C=C bond in aromatic ring and it

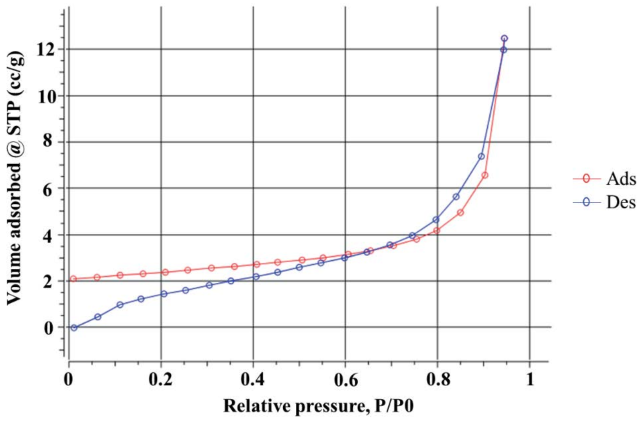

Fig. 2. N_2 adsorption–desorption isotherm of palm leaves.

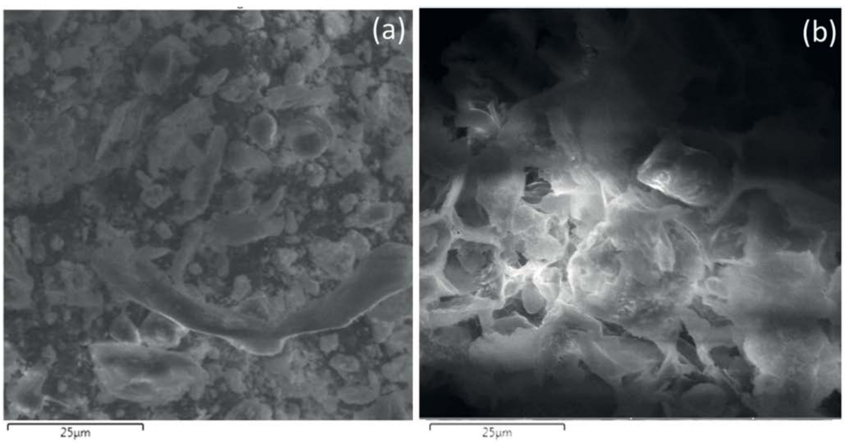

Fig. 3. SEM image of palm leave (a) before and (b) after Pb(II) adsorption.

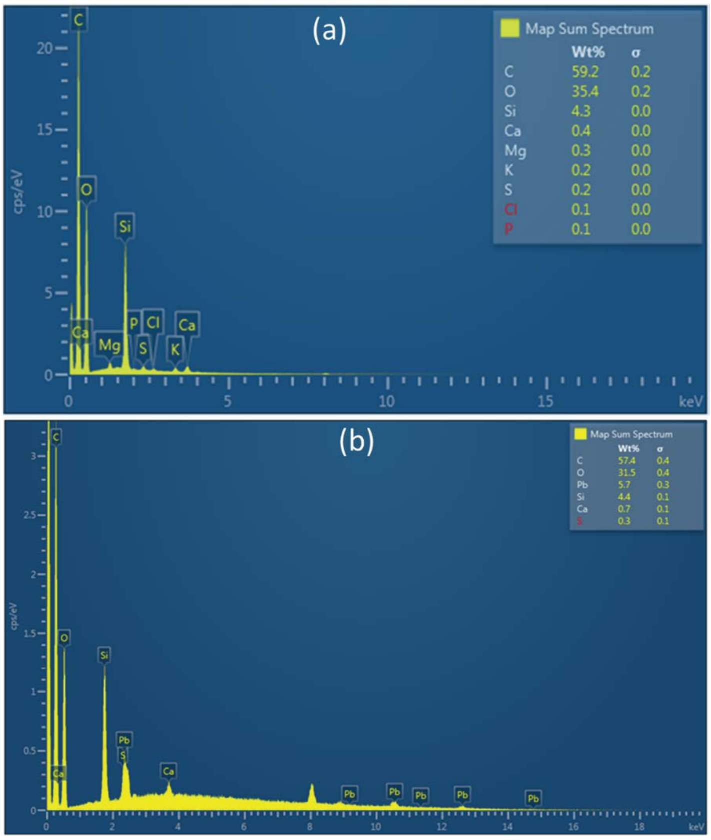

Fig. 4. EDS mapping of palm leave before (a) and after (b) Pb(II) adsorption.

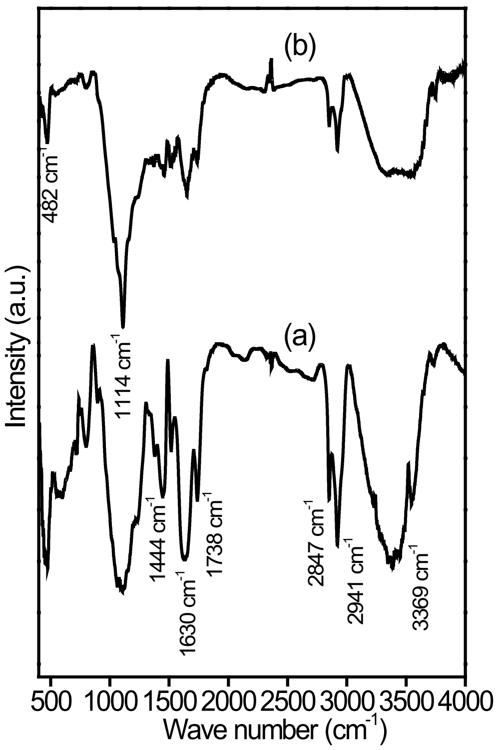

Fig. 5. FTIR spectrum of palm leaves (a) before and (b) after Pb(II) adsorption.

can also represent H–O–H bending band of water [40,41]. The peak at 1,444 cm^{-1} is attributed to aliphatic C–H, the peak located at 1,114 cm^{-1} is assigned to C–O–C in cellulose and hemicelluloses. The peak in between 484 cm^{-1} are related to aromatic C–H groups of palm leaves [38]. After Pb adsorption (Fig. 5b), it can be seen that the –OH peak intensity significantly decreased which implies that –OH functional groups involved in adsorption process via ion exchange and some peaks wavenumber slightly changed which indicates that oxygen containing functional groups coordinating with Pb(II) via ion exchange, complexation process. Moreover, in Fig. 5b a new peak was noticed at 802 cm^{-1} is related to Pb–O bond.

The XRD patter of palm leaves before and after adsorption are illustrated in Fig. 6a and b. The profiles of palm leaves samples were used to study the deterioration level and the changes in crystallinity level before and after Pb(II) adsorption. XRD patterns of the fresh sample (Fig. 6a) shows the two kinds of cellulose, that is, amorphous cellulose at 2q = 16.7 and crystalline cellulose at 2q = 21.6, and less intensity peak at 2q = 34.5 is assigned the hemicelluloses [42], but lignin does not show any diffraction peaks, but diffuse scattering halos in the 2q range from 12 to 27, which overlap with the crystalline diffraction peak positions [38,43]. Four major peaks at 2q = 14.5, 16.5, 22.6, and 34.52 were related to (101), (101), (002), and (040) crystallographic planes, respectively. Surprisingly, there are no structural changes after Pb(II) (Fig. 6b) which implies that the adsorbent material is stable in water solution.

3.2. Influence of adsorption parameters

It is crucial to demonstrate the effect of operating factors such as contact time, mass of adsorbent, initial concentration of Pb(II) in an aqueous solution, temperature and pH on the removal of Pb(II) by using palm leaves from an aqueous solution. The effect of contact time on the Pb(II) removal from an aqueous solution is depicted in Fig. 7a. As seen in this figure, the removal efficiency suddenly increased to 66% within the first 10 min due to the availability of active adsorption sites onto the adsorbent surface and the interaction between Pb(II) molecules and the surface of the palm leaves. With time the removal efficiency slowly increased from 66% at 10 min to 75.9% at 360 min. Next, no major changes were observed in the removal efficiency with time, the removal efficiency was 76.2% at 1,440 min. The slower increase in removal efficiency after 10 min attributed to the diffusion of Pb(II) ions into the internal pores of the adsorbent. However, after 360 min, the equilibrium has been achieved and few particles found a places to be adsorbed. Hence, the time 360 could be assumed the equilibrium time of Pb(II) removal by palm leaves.

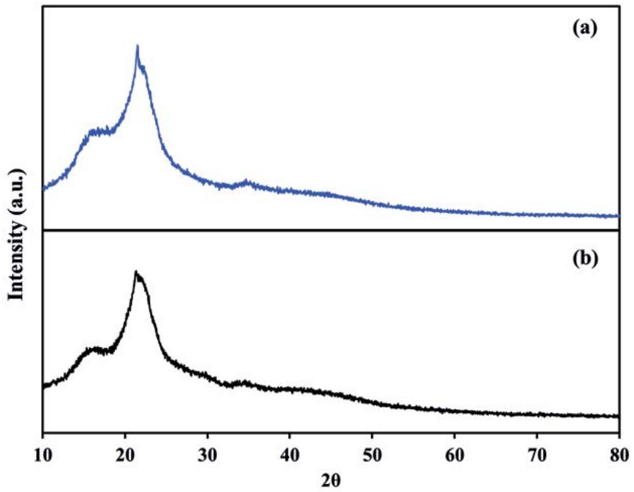

Fig. 6. XRD pattern of palm leaves (a) before and (b) after Pb(II) adsorption.

The mass of adsorbent has an important impact on metal ions removal from an aqueous solution. The influence of the mass of palm leaves on the removal efficiency of Pb(II) from an aqueous solution is denoted in Fig. 7b. The removal efficiency found to enhance from 52% to 93% with increase in mass of palm leaves 0.01 to 0.06 g. It was associated to increase in number of adsorption sites with increasing mass of palm leaves [44]. Hence, it can be said that for an initial concentration of 30 mg/L of Pb(II) ions, more than 90% can be removed using 1.5 g (palm leaves) per liter of solution.

Fig. 7c shows the effect of initial concentration of Pb(II) on the removal of Pb(II) from an aqueous solution. It was noted that the removal efficiency was decreasing by rising the initial concentration of Pb(II) ions. For instance, the removal efficiency was 16% and 76% for an initial concentration of 500 and 30 mg/L, respectively. This trend might be ascribed to the saturation of the adsorbent with adsorbate molecules at low concentration of Pb(II) ions. And hence, further increasing the initial concentration of Pb(II)

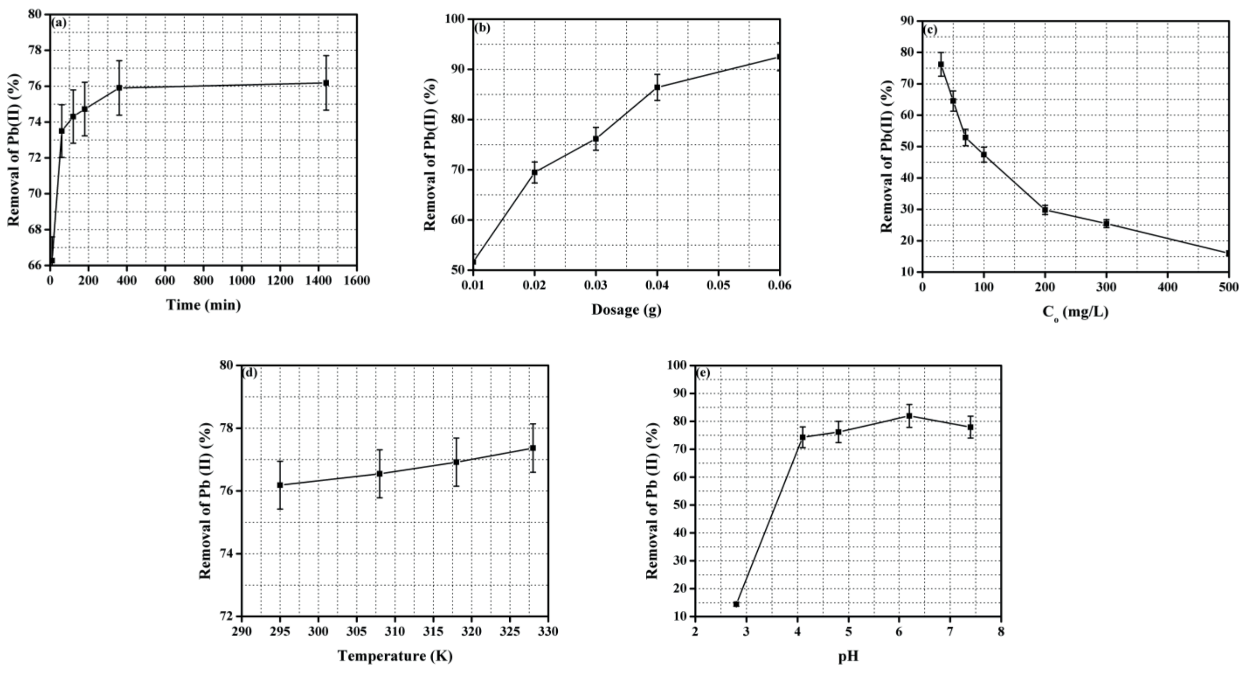

Fig. 7. (a) Effect of contact time, (b) dosage, (c) initial concentration, (d) temperature, (e) pH on the percentage removal of Pb(II) by using palm leaves from an aqueous solution. Sample volume 20 mL, agitation speed 200 rpm. Detailed experimental conditions are provided in Table 1.

ions against a constant dose of palm leaves will keep some of metal ion unabsorbed that results in decreased removal efficiency.

It is significant to explore the influence of temperature on the adsorption of Pb(II) from an aqueous solution onto palm leaves. The effect of temperature on the removal of P(II) is shown in Fig. 7d. The removal efficiency of P(II) ions was found to be enhanced from 76% to 77% by increasing the temperature from 22°C to 55°C. It was due to acceleration of some originally slow adsorption stages or to the creation of some new active sites on the surface of palm leaves [25]. Moreover, increasing the temperature might increase the mobility of Pb(II) ions allowing them to pass through the pores of the adsorbent which in turn increase the removal efficiency. Results indicated that Pb(II) adsorption onto palm leaves is an endothermic process.

The pH of the medium influences significantly the Pb(II) adsorption onto palm leaves and it is a crucial endowment. By fluctuating the pH of the solution, the chemical speciation, metal ions solubility, and counter ions concentration on the functional groups of the adsorbents influenced [25,26]. Fig. 7e shows effect of the initial solution pH on the removal of Pb(II) by palm leaves. The effect of pH is always cross-linked with the pH_{PZC} of the adsorbent [45]. The pH_{PZC} of the palm leaves was found to be 5.3 and the results are illustrated in Fig. 8. The adsorption results demonstrated an increase in the removal efficiency from 14% to 82% by increasing the solution pH from 2.8 to 6.2. These results are attributed to the surface charge of the adsorbent, at low pH (pH 2.8), the adsorbent is positively charged and the Pb(II) ions are positively charged and hence low removal efficiency was achieved (14.4%). Increasing the solution pH from 2.8 to 4.8 has resulted in an increase in the removal efficiency to 76.2%. This trend is attributed to the reduction in H^+ ions by increasing the solution pH which in turn decrease the magnitude of the positive charge in the adsorbent and hence decrease the magnitude of the electrostatic repulsions which at the ends resulted in improved removal efficiency. Further increase the solution pH to 6.2, the removal efficiency increased to 82%. It is worth mentioning that this pH value (6.2) exceeded the pH_{PZC} (5.3) of the adsorbent, which means that the adsorbent now is negatively charged. Hence, the positively charged Pb(II) ions are getting adsorbed by the negatively charged palm leaves by electrostatic interactions, which explains the increase in the removal efficiency. Next, at pH 7.4, the removal efficiency slightly decreased to 77.9%, at this pH, Pb(II) ions started to precipitate as lead hydroxides and resulted in decreased removal efficiency [46].

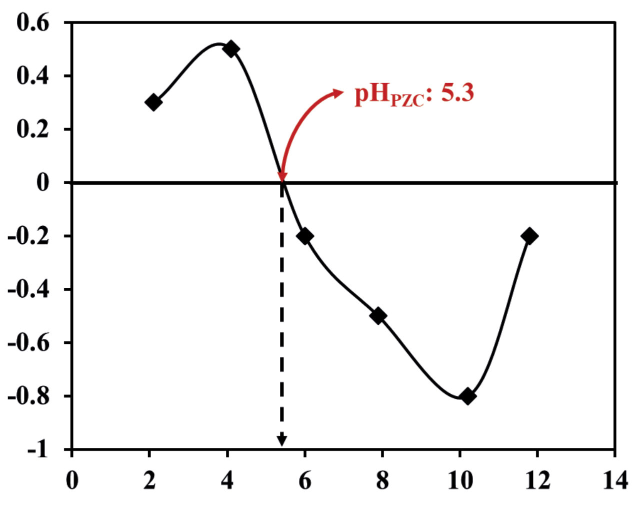

Fig. 8. pH_{PZC} of palm leaves powder.

3.3. Adsorption kinetics

Pb(II) adsorption kinetics was investigated by applying several models including pseudo-first-order, pseudo-second-order, Elovich model, liquid film diffusion model, modified Freundlich equation and Bangham equation. Fig. 9a shows the plot of pseudo-first-order model for Pb(II) adsorption onto palm leaves and the values of its parameters are given in Table 2. The R^2 = 0.995 value was close to unity. On the other hand, there was a large difference between the values of calculated and experimental adsorption capacity. Therefore, pseudo-first-order model can't explain Pb(II) adsorption onto palm leaves. Fig. 9b depicts the plot of pseudo-second-order for Pb(II) adsorption and the measured values of its parameters are shown in Table 2. It can be seen that the value of experimental and calculated adsorption capacity were very close to each other (Table 2). The R^2 value is 1 indicating that Pb(II) adsorption fitted well to pseudo-second-order model. The Elovich and modified Freundlich models were applied to further investigate the dynamic mechanism of Pb(II) ions removal onto the palm leaves. The linearized plots of these models are demonstrated in Fig. 9c and e, respectively, the values of R^2 and model parameters are presented in Table 2. The value of R^2 of the two models were between 0.766 and 0.850 suggesting that these models didn't fit the kinetic data.

To further investigate the adsorption mechanism of Pb(II) ions by palm leaves, the liquid film diffusion model was applied. If the linearized kinetic data form a straight line with respect to the liquid film diffusion model equation and pass through the origin, then the adsorption process is controlled by the diffusion of Pb(II) ions through the liquid film around the palm leaves particles. Fig. 9d illustrates that the data form a straight line with R^2 of 0.995, however the straight line didn't pass through the origin which indicates that that the diffusion of the Pb(II) ions through the liquid film around the palm leaves powder was not the rate-determining step.

Moreover, the Bangham kinetic equation was applied on the kinetic data and the linearized plot is given in Fig. 9f. If the linearized kinetic data forms a straight line using the Bangham equation, then it can be said that the internal pore diffusion is the controlling mechanism of the adsorption process. As seen in Fig. 9f, the linearized data didn't form a straight line with R^2 of 0.753 implying that the diffusion of Pb(II) into pores of the palm leaves is not the only rate controlling step [33,47]. It may be that both film and pore diffusion were crucial in Pb(II) adsorption from an aqueous solution to different extent.

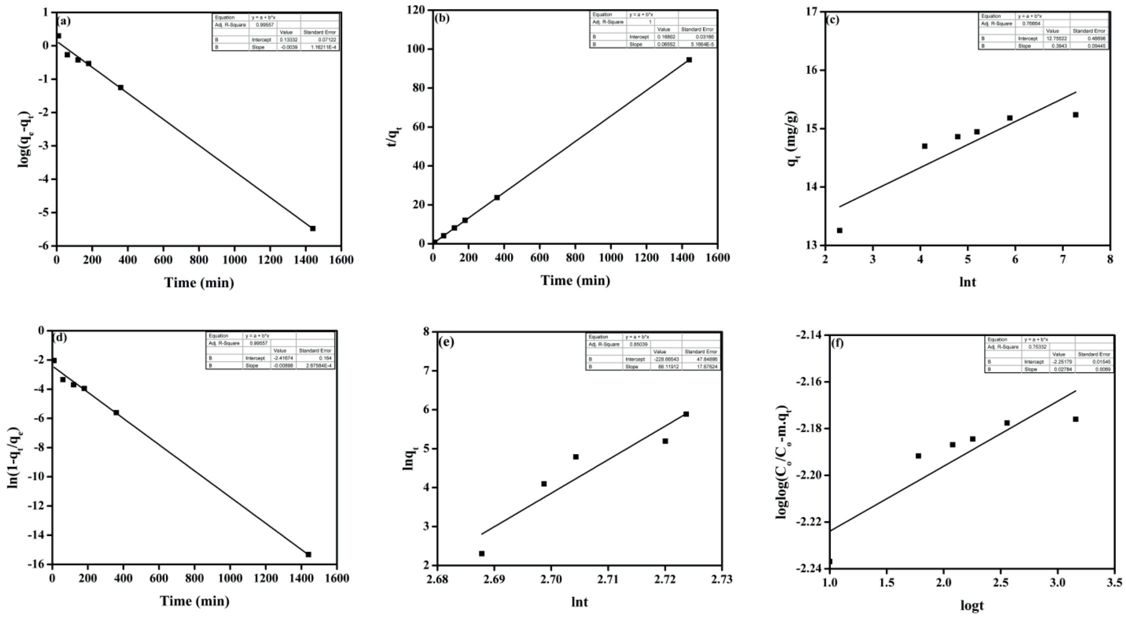

Fig. 9. (a) Pseudo-first-order model, (b) pseudo-second-order model, (c) Elovich model, (d) liquid-film diffusion model, (e) modified Freundlich equation, (f) Bangham equation for Pb(II) adsorption onto palm leaves from aqueous solution. Kinetic experiment conditions: contact time 1–1,440 min, initial Pb(II) concentration: 30 mg/L, temperature: 22°C, initial solution pH 4.8, palm leaves dosage 0.03 g.

Table 2
The calculated values kinetics parameters for Pb(II) adsorption onto palm leaves from an aqueous solution

Kinetic models	Parameters	
	$q_{e(\text{exp.})}$	15.2
	$q_{e(\text{cal.})}$	1.40
Pseudo-first-order model	$k_1 \times 10^{-3}$	3.90
	R^2	0.995
	q_e	15.30
Pseudo-second-order model	$k_2 \times 10^{-3}$	25.50
	R^2	1.00
	$\alpha \times 10^{-13}$	4.0
Elovich model	β	2.5
	R^2	0.766
	$k_{fd} \times 10^{-3}$	8.98
Liquid-film diffusion model	C_{fd}	–2.42
	R^2	0.995
	$M \times 10^{-3}$	11.6
Modified Freundlich equation	$k \times 10^{-101}$	1.64
	R^2	0.850
	k_0	3.32
Bangham equation	α	0.078
	R^2	0.753

q_e (mg/g); k_1 (min^{-1}); k_2 (g/mg min); α (mg/g min); β (g/mg); k_{fd} (min^{-1}); k (L/g min); k_0 (mL/g/L), parameters explanations are given in Section S1.

3.4. Adsorption isotherms

Adsorption isotherm models including Langmuir, Freundlich, Temkin, and Dubinin–Radushkevich were used to demonstrate Pb(II) adsorption onto palm leaves. For Pb(II) adsorption onto palm leaves, Langmuir adsorption isotherm is shown in Fig. 10a and the measured values of its parameters are given in Table 3. The correlation coefficient (R^2 = 0.990) value was close to unity denoting that Pb(II) adsorption onto palm leaves obeyed to Langmuir isotherm. In addition, the value of the separation factor (R_L) was between 0.068 and 0.552 implying that the Pb(II) adsorption was favorable onto palm leaves. Fig. 10b indicates Freundlich isotherm for Pb(II) adsorption onto palm leaves and the measured values of its parameters are given in Table 3. The correlation coefficient (R^2 = 0.926) value showed that Pb(II) adsorption obeyed to Freundlich isotherm. Nevertheless, the of Freundlich constant 'n' value ranges from 2–10 represented good adsorption, 1–2 moderate adsorption and less than one showed poor adsorption [27,33,47]. Temkin isotherm for Pb(II) adsorption is shown in Fig. 10c and the attained values of b_T and A_T are shown Table 3. The correlation coefficient (R^2 = 0.811) value was lower than Langmuir isotherm indicating that Pb(II) adsorption was not followed it. Fig. 10d represents Dubinin–Radushkevich isotherm for Pb(II) adsorption and the values of D–R isotherm parameters are given in Table 3. The determined value mean adsorption energy was 0.760 KJ/mol denoting that Pb(II) adsorption was physical adsorption process. It should be mentioned that the maximum adsorption capacity of Pb(II) onto palm leaves was 57.4 mg/g which is higher than most of the bio adsorbents listed in Table 4.

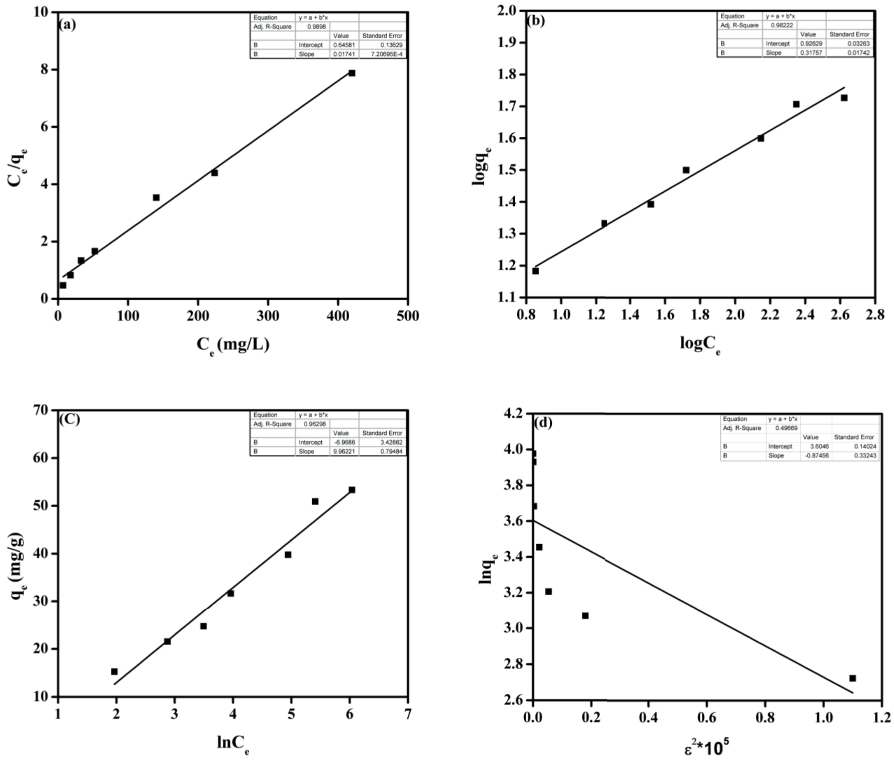

Fig. 10. (a) Langmuir, (b) Freundlich, (c) Temkin, (d) Dubinin–Radushkevich iostherm for Pb(II) adsorption onto palm leaves from an aqueous solution. Isotherm experimental conditions: initial Pb(II) concentration 30–500 mg/L, temperature 22°C, contact time 1,440 min, palm leaves dosage 0.03 g, initial solution pH 4.8.

Table 3
The determined values of isotherm parameters for Pb(II) adsorption from onto palm leaves from an aqueous solution

Adsorption isotherms	Parameters	
Langmuir isotherm	Q_m	57.40
	K_L	0.027
	R_L	0.068–0.552
	R^2	0.990
Freundlich isotherm	n	3.15
	K_f	8.44
	R^2	0.926
Temkin isotherm	b_T	248.60
	A_T	0.50
	R^2	0.963
Dubinin–Radushkevich isotherm	β	0.87
	C_m	36.80
	R^2	0.496
	E	0.760

Q_m (mol/g); K_L (L/mol); K_f((mg/g)(L/mg)$^{1/n}$); C_m (mol/g); β (mol^2/J^2), E (kJ/mol), parameters explanations are given in Section S2.

3.5. Adsorption thermodynamics

For the investigation of heat change, spontaneity, and feasibility of the adsorption process onto the surface of adsorbent and adsorption mechanism, thermodynamic study is significant [22]. The thermodynamic parameters determination procedure and detailed parameters are provided in Section S3. Fig. 11 denotes the plot of lnK_c vs. 1/T for Pb(II) adsorption onto palm leaves. The values of ΔG°, ΔH°, and ΔS° were determined to study adsorption thermodynamics and are given in Table 5. The degree of randomness at the adsorbent–adsorbate interface was increased due to the positive value of ΔS° for Pb(II) adsorption onto palm leaves [22,47]. For Pb(II) adsorption onto palm leaves, the attained value of ΔH° was positive. It demonstrated that Pb(II) adsorption onto palm leaves was endothermic adsorption process [57,58]. Contrary, the negative value of ΔG° represented that Pb(II) adsorption onto palm leaves was spontaneous in nature. Adsorption of Pb(II) was favored at room temperature than at higher temperatures as shown by the enhancement in values of ΔG° with increase in temperature.

3.6. Reusability studies

Desorption experiments were then conducted to evaluate the regeneration of palm leaves after Pb(II) adsorption. The palm leaves were tested for the removal of Pb(II) ions in 5 consecutive adsorption/desorption cycles. The removal efficiency against the number of adsorption/desorption cycles is presented in Fig. 12. As shown in this figure, the removal efficiency was decreased from 92.5% in the first adsorption experiment to 59.2% after 5 adsorption/desorption cycles. The decrease in the removal efficiency with adsorption/desorption cycles might be attributed to loss of some palm leaves powder during the washing process

Table 4
Maximum Pb(II) adsorption capacity onto selected bio adsorbents

Adsorbents	Investigated Pb(II) concentration (mg/L)	Maximum adsorption capacity (mg/g)	Reference
Palm leaves	30–500	57.4	This study
Pine (*Pinus halepensis*) sawdust	1–50	13.5	[48]
Ficus benghalensis leaves	0–100	28.6	[49]
Oil palm bio-waste/MWCNTs reinforced PVA hydrogel composite	65–200	30.0	[50]
Mucilaginous leaves of *Diceriocaryum eriocarpum* Plant	1–50	41.5	[51,52]
Grape stalk waste	49.7–629.3	79.8	[53,54]
Hazelnut ground shells	10–200	16.5	[55]
Almond ground shell	10–200	5.5	[55]
Olive cake	0–>900	19.5	[56]
Raw and treated *Rosa bourbonia* waste phyto-biomass	25–400	68.5–72.0	[51]
Native and immobilized *Mangifera indica* biomass	25–400	143–151	[53]

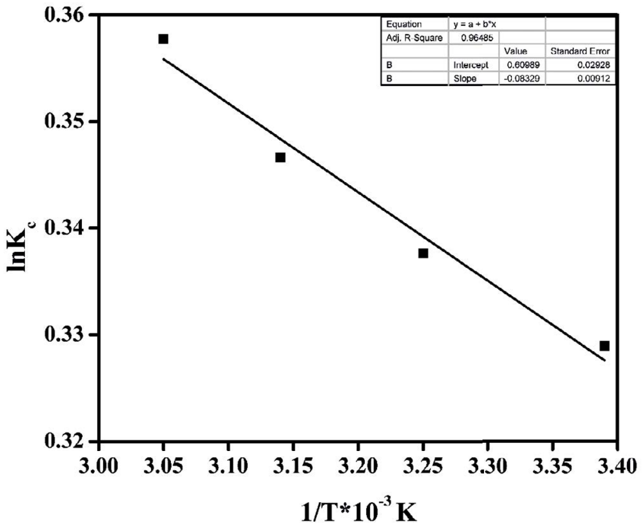

Fig. 11. Plot of lnK_c vs. 1/T for Pb(II) adsorption onto palm leaves from an aqueous solution. Temperature 22°C–55°C, initial Pb(II) concentration: 30 mg/L, contact time 1,440 min, initial solution pH 4.8, palm leaves dosage 0.03 g.

Table 5
The value thermodynamic factors for Pb(II) adsorption onto palm leaves from aqueous solution

Temperature (K)	ΔH (kJ/mol)	ΔS (J/K. mol)	ΔG (kJ/mol)
295	1.60	11.70	–1.85
308			–1.99
318			–2.11
328			–2.25

Temperature 22°C–55°C, initial Pb(II) concentration: 30 mg/L, contact time 1,440 min, initial solution pH 4.8, palm leaves dosage 0.03 g.

with HCl and deionized water. Moreover, some Pb(II) ions might adsorbed through a chemical bonding onto the surface of the palm leaves and couldn't be removed during the desorption process which in turn reduce the removal efficiency in the next adsorption experiment. Furthermore, the functional groups onto the surface of the palm leaves might be affected during the HCl washing and hence it affects the removal efficiency in the coming adsorption experiment. However, more than 59% of an initial concentration of 30 mg/L of lead ions can still be achieved after 5 adsorption/desorption cycles. These results suggesting that palm leaves are a promising bio adsorbent for Pb(II) ions elimination from an aqueous solution.

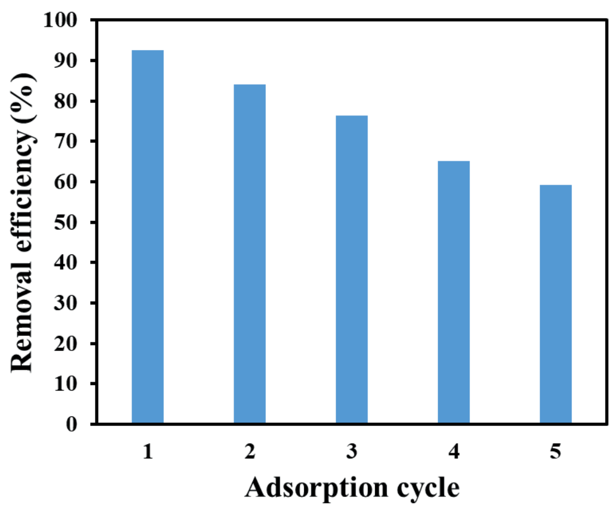

Fig. 12. Removal efficiency of Pb(II) ions onto palm leaves against the number of adsorption/desorption experiments.

4. Conclusions

In the current work, the adsorptive removal of Pb(II) ions from synthetic water by palm leaves powder was investigated by batch mode experiments. The textural characterization of the adsorbent demonstrated a mesoporous material with a surface area of 3.6 m^2/g. The FTIR and EDS mapping of the spent adsorbent illustrated the successful removal of Pb(II) ions by palm leaves. According to

FTIR analysis and the influence of pH study, the adsorption process was dominated by electrostatic interactions, ion exchange, and complexation mechanisms. Palm leaves have shown to provide a maximum adsorption capacity of 57.4 mg/g according to Langmuir isotherm modeling. The kinetics found to fit well with pseudo-second-order kinetic model with R^2 of 1. The thermodynamics analysis elucidated a feasible, spontaneous and endothermic adsorption process. The palm leaves found to achieve equilibrium in 360 min suggesting a fast removal of Pb(II) ions by this adsorbent. Moreover, the palm leaves found to provide a removal efficiency of more than 59% after 5 adsorption/desorption cycles using 1 g/L of palm leaves and 30 mg/L of Pb(II) ions. Hence, the palm leaves could be a promising material in the remediation of heavy metals from an aqueous solutions.

Acknowledgement

The authors are highly thankful to University of Sharjah (UOS), Sharjah, United Arab Emirates for financial support.

References

[1] R.L. Canfield, C.R. Henderson, D.A. Cory-Slechta, C. Cox, T.A. Jusko, B.P. Lanphear, Intellectual impairment in children with blood lead concentrations below 10 µg per deciliter, New England J. Med., 348 (2003) 1517–1526.

[2] K.N.D.A. Chen, J.H.Ware, J. Radcliffe, W.J. Rogan, IQ and blood lead from 2 to 7 years of age: are the effects in older children the residual of high blood lead concentrations in 2-year-olds?, Environ. Health Perspect., 113 (2005) 597–601.

[3] S.Wang, J. Zhang, Blood lead levels in children, China, Environ. Res., 101 (2006) 412–418.

[4] R. Jalali, H. Ghafourian, Y. Asef, S.J. Davarpanah, S. Sepehr, Removal and recovery of lead using nonliving biomass of marine algae, J. Hazard. Mater., 92 (2002) 253–262.

[5] P. Gottesfeld, Time to ban lead in industrial paints and coatings, Front. Public Health, 3 (2015) 144, doi: 10.3389/fpubh.2015.00144.

[6] J.D. Weidenhamer, P.A. Kobunski, G. Kuepouo, R.W. Corbin, P. Gottesfeld, Lead exposure from aluminum cookware in Cameroon, Sci. Total Environ., 496 (2014) 339–347.

[7] N. Arancibia-Miranda, S.E. Baltazar, A. García, D. Muñoz-Lira, P. Sepúlveda, M.A. Rubio, D. Altbir, Nanoscale zero valent supported by zeolite and montmorillonite: template effect of the removal of lead ion from an aqueous solution, J. Hazard. Mater., 301 (2016) 371–380.

[8] J. Cruz-Olivares, G. Martínez-Barrera, C. Pérez-Alonso, C.E. Barrera-Díaz, M. del C. Chaparro-Mercado, F. Ureña-Núñez, Adsorption of lead ions from aqueous solutions using gamma irradiated minerals, J. Chem., 2016 (2016) 8782469, doi: 10.1155/2016/8782469.

[9] M. Iqbal, *Vicia faba* bioassay for environmental toxicity monitoring: a review, Chemosphere, 144 (2016) 785–802.

[10] M. Abbas, M. Adil, S. Ehtisham-ul-Haque, B. Munir, M. Yameen, A. Ghaffar, G.A. Shar, M. Asif Tahir, M. Iqbal, *Vibrio fischeri* bioluminescence inhibition assay for ecotoxicity assessment: a review, Sci. Total Environ., 626 (2018) 1295–1309.

[11] N. Ferronato, V. Torretta, Waste mismanagement in developing countries: a review of global issues, Int. J. Environ. Res. Public Health, 16 (2019) 1060.

[12] M. Alsuhybani, A. Alshahrani, M. Algamdi, A.A. Al-Kahtani, A.A. Alqadami, Highly efficient removal of Pb(II) from aqueous systems using a new nanocomposite: adsorption, isotherm, kinetic and mechanism studies, J. Mol. Liq., 301 (2020) 112393.

[13] X. Huang, D. Wei, X. Zhang, D. Fan, X. Sun, B. Du, Q. Wei, Synthesis of amino-functionalized magnetic aerobic granular sludge-biochar for Pb(II) removal: adsorption performance and mechanism studies, Sci. Total Environ., 685 (2019) 681–689.

[14] M. Naushad, Z.A. Alothman, Separation of toxic Pb^{2+} metal from aqueous solution using strongly acidic cation-exchange resin: analytical applications for the removal of metal ions from pharmaceutical formulation, Desal. Water Treat., 53 (2015) 2158–2166.

[15] H. Ali, E. Khan, I. Ilahi, Environmental chemistry and ecotoxicology of hazardous heavy metals: environmental persistence, toxicity, and bioaccumulation, J. Chem., 2019 (2019) 6730305.

[16] F. Ferella, M. Prisciandaro, I. De Michelis, F. Veglio', Removal of heavy metals by surfactant-enhanced ultrafiltration from wastewaters, Desalination, 207 (2007) 125–133.

[17] V.V.K. Goncharuk, B.Y. Pavlenko, V.M. Babak, M.I. Pshinko, G.N. Pysmennyi, Uranium compounds purification from water and wastewater, J. Water Chem. Technol., 23 (2001) 44.

[18] D. Mohan, S. Chander, Single component and multi-component adsorption of metal ions by activated carbons, Colloids Surf., A, 177 (2001) 183–196.

[19] J.S. Kim, C.H. Lee, S.H. Han, M.Y. Suh, Studies on complexation and solvent extraction of lanthanides in the presence of diaza-18-crown-6-di-isopropionic acid, Talanta, 45 (1997) 437–444.

[20] Z. Reddad, C. Gerente, Y. Andres, P. Le Cloirec, Adsorption of several metal ions onto a low-cost biosorbent: kinetic and equilibrium studies, Environ. Sci. Technol., 36 (2002) 2067–2073.

[21] N. Ünlü, M. Ersoz, Adsorption characteristics of heavy metal ions onto a low cost biopolymeric sorbent from aqueous solutions, J. Hazard. Mater., 136 (2006) 272–280.

[22] M.I. Khan, A. Shanableh, J. Fernandez, M.H. Lashari, S. Shahida, S. Manzoor, S. Zafar, A. Rehman, N. Elboughdiri, Synthesis of DMEA-grafted anion exchange membrane for adsorptive discharge of methyl orange from wastewaters, Membranes, 11 (2021) 166.

[23] M.I. Khan, A. Shanableh, N. Nasir, S. Shahida, Adsorptive removal of methyl orange from wastewaters by the commercial anion exchange membrane EPTAC, Desal. Water Treat., 234 (2021) 245–254.

[24] S. Zafar, M.I. Khan, W. Hassan, S. Mubeen, T. Javed, S. Shahida, S. Manzoor, A. Shanableh, M.L. Mirza, A. Rehman, N. Khalid, M.H. Lashari, Application of NaOH-treated rice husk for adsorptive discharge of cobalt ions from wastewater, Desal. Water Treat., 226 (2021) 328–338.

[25] S. Zafar, M.I. Khan, A. Shanableh, S. Ahmad, S. Manzoor, S. Shahida, P. Prapamonthon, S. Mubeen, A. Rehman, Adsorption of silver, thorium and nickel ions from aqueous solution onto rice husk, Desal. Water Treat., 236 (2021) 108–122.

[26] S. Zafar, M.I. Khan, H. Rehman, J. Fernandez-Garcia, S. Shahida, P. Prapamonthon, M. Khraisheh, A. Rehman, H.B. Ahmad, M.L. Mirza, N. Khalid, M.H. Lashari, Kinetic, equilibrium, and thermodynamic studies for adsorptive removal of cobalt ions by rice husk from aqueous solution, Desal. Water Treat., 204 (2020) 285–296.

[27] S. Zafar, M.I. Khan, M. Khraisheh, M.H. Lashari, S. Shahida, M.F. Azhar, P. Prapamonthon, M.L. Mirza, N. Khalid, Kinetic, equilibrium and thermodynamic studies for adsorption of nickel ions onto husk of *Oryza sativa*, Desal. Water Treat., 167 (2019) 277–290.

[28] H. Mohammadifard, M.C. Amiri, Evaluating Cu(II) removal from aqueous solutions with response surface methodology by using novel synthesized $CaCO_3$ nanoparticles prepared in a colloidal gas aphron system, Chem. Eng. Commun., 204 (2017) 476–484.

[29] A.A. Alswat, M.B. Ahmad, T.A. Saleh, Zeolite modified with copper oxide and iron oxide for lead and arsenic adsorption from aqueous solutions, J. Water Supply Res. Technol. AQUA, 65 (2016) 465–479.

[30] H.A. Sani, M.B. Ahmad, T.A. Saleh, Synthesis of zinc oxide/talc nanocomposite for enhanced lead adsorption from aqueous solutions, RSC Adv., 6 (2016) 108819–108827.

[31] T.A. Saleh, V.K. Gupta, A.A. Al-Saadi, Adsorption of lead ions from aqueous solution using porous carbon derived from rubber tires: experimental and computational study, J. Colloid Interface Sci., 396 (2013) 264–269.

[32] S. Zafar, M.I. Khan, M. Khraisheh, S. Shahida, N. Khalid, M.L. Mirza, Effective removal of lanthanum ions from aqueous solution using rice husk: impact of experimental variables, Desal. Water Treat., 132 (2019) 263–273.
[33] S. Zafar, M. Khan, M. Khraisheh, S. Shahida, T. Javed, M.L. Mirza, N. Khalid, Use of rice husk as an efective sorbent for the removal of cerium ions from aqueous solution: kinetic, equilibrium and thermodynamic studies, Desal. Water Treat., 150 (2019) 124–135.
[34] S. Zafar, M.I. Khan, M.H. Lashari, M. Khraisheh, F. Almomani, M.L. Mirza, N. Khalid, Removal of copper ions from aqueous solution using NaOH-treated rice husk, Emergent Mater., (2020), doi: 10.1007/s42247-020-00126-w.
[35] I.W. Almanassra, V. Kochkodan, G. Ponnusamy, G. McKay, M. Ali Atieh, T. Al-Ansari, Carbide derived carbon (CDC) as novel adsorbent for ibuprofen removal from synthetic water and treated sewage effluent, J. Environ. Health Sci. Eng., 18 (2020) 1375–1390.
[36] A.K.A. Khalil, F. Dweiri, I.W. Almanassra, A. Chatla, M.A. Atieh, Mg-Al layered double hydroxide doped activated carbon composites for phosphate removal from synthetic water: adsorption and thermodynamics studies, Sustainability, 14 (2022) 6991.
[37] M.I. Khan, A. Shanableh, Adsorption of Rhodamine B from an aqueous solution onto NaOH-treated rice husk, Desal. Water Treat., 254 (2022) 104–115.
[38] I. Ben Salem, M. El Gamal, M. Sharma, S. Hameedi, F.M. Howari, Utilization of the UAE date palm leaf biochar in carbon dioxide capture and sequestration processes, J. Environ. Manage., 299 (2021) 113644.
[39] C.H. Chia, B. Gong, S.D. Joseph, C.E. Marjo, P. Munroe, A.M. Rich, Imaging of mineral-enriched biochar by FTIR, Raman and SEM–EDX, Vib. Spectrosc., 62 (2012) 248–257.
[40] H. Zhang, T. Lu, M. Wang, R. Jin, Y. Song, Y. Zhou, Z. Qi, W. Chen, Inhibitory role of citric acid in the adsorption of tetracycline onto biochars: effects of solution pH and Cu^{2+}, Colloids Surf., A, 595 (2020) 124731.
[41] B. Sizirici, Y.H. Fseha, I. Yildiz, T. Delclos, A. Khaleel, The effect of pyrolysis temperature and feedstock on date palm waste derived biochar to remove single and multi-metals in aqueous solutions, Sustainable Environ. Res., 31 (2021) 9.
[42] J. Gong, J. Li, J. Xu, Z. Xiang, L. Mo, Research on cellulose nanocrystals produced from cellulose sources with various polymorphs, RSC Adv., 7 (2017) 33486–33493.
[43] A. Boukir, S. Fellak, P. Doumenq, Structural characterization of *Argania spinosa* Moroccan wooden artifacts during natural degradation progress using infrared spectroscopy (ATR-FTIR) and X-Ray diffraction (XRD), Heliyon, 5 (2019) e02477.
[44] I.W. Almanassra, V. Kochkodan, M. Subeh, G. McKay, M. Atieh, T. Al-Ansari, Phosphate removal from synthetic and treated sewage effluent by carbide derive carbon, J. Water Process Eng., 36 (2020) 101323.
[45] I.W. Almanassra, V. Kochkodan, G. McKay, M.A. Atieh, T. Al-Ansari, Kinetic and thermodynamic investigations of surfactants adsorption from water by carbide-derived carbon, J. Environ. Sci. Health, Part A, 56 (2021) 1206–1220.
[46] X. Guan, X. Yuan, Y. Zhao, J. Bai, Y. Li, Y. Cao, Y. Chen, T. Xiong, Adsorption behaviors and mechanisms of Fe/Mg layered double hydroxide loaded on bentonite on Cd(II) and Pb(II) removal, J. Colloid Interface Sci., 612 (2022) 572–583.
[47] M.I. Khan, M.H. Lashari, M. Khraisheh, S. Shahida, S. Zafar, P. Prapamonthon, A. Rehman, S. Anjum, N. Akhtar, F. Hanif, Adsorption kinetic, equilibrium and thermodynamic studies of Eosin-B onto anion exchange membrane, Desal. Water Treat., 155 (2019) 84–93.
[48] L. Semerjian, Removal of heavy metals (Cu, Pb) from aqueous solutions using pine (*Pinus halepensis*) sawdust: equilibrium, kinetic, and thermodynamic studies, Environ. Technol. Innovation, 12 (2018) 91–103.
[49] V.R. Surisetty, J. Kozinski, L. Rao Nageswara, Biosorption of lead ions from aqueous solution using *Ficus benghalensis* L., J. Eng., 2013 (2013) 167518.
[50] M. Zulfiqar, S.Y. Lee, A.A. Mafize, N.A.M.A. Kahar, K. Johari, N.E. Rabat, Efficient removal of Pb(II) from aqueous solutions by using oil palm bio-waste/MWCNTs reinforced PVA hydrogel composites: kinetic, isotherm and thermodynamic modeling, Polymers, 12 (2020) 430.
[51] Q. Manzoor, R. Nadeem, M. Iqbal, R. Saeed, T.M. Ansari, Organic acids pretreatment effect on *Rosa bourbonia* phyto-biomass for removal of Pb(II) and Cu(II) from aqueous media, Bioresour. Technol., 132 (2013) 446–452.
[52] J.N. Edokpayi, J.O. Odiyo, T.A.M. Msagati, E.O. Popoola, A novel approach for the removal of lead(II) ion from wastewater using mucilaginous leaves of *Diceriocaryum eriocarpum* plant, Sustainability, 7 (2015) 14026–14041.
[53] R. Nadeem, Q. Manzoor, M. Iqbal, J. Nisar, Biosorption of Pb(II) onto immobilized and native *Mangifera indica* waste biomass, J. Ind. Eng. Chem., 35 (2016) 185–194.
[54] M. Martínez, N. Miralles, S. Hidalgo, N. Fiol, I. Villaescusa, J. Poch, Removal of lead(II) and cadmium(II) from aqueous solutions using grape stalk waste, J. Hazard. Mater., 133 (2006) 203–211.
[55] Y. Bulut, Z. Tez, Adsorption studies on ground shells of hazelnut and almond, J. Hazard. Mater., 149 (2007) 35–41.
[56] S. Doyurum, A. Çelik, Pb(II) and Cd(II) removal from aqueous solutions by olive cake, J. Hazard. Mater., 138 (2006) 22–28.
[57] I.W. Almanassra, G. McKay, V. Kochkodan, M. Ali Atieh, T. Al-Ansari, A state of the art review on phosphate removal from water by biochars, Chem. Eng. J., 409 (2021) 128211.
[58] I.W. Almanassra, V. Kochkodan, G. McKay, M.A. Atieh, T. Al-Ansari, Review of phosphate removal from water by carbonaceous sorbents, J. Environ. Manage., 287 (2021) 112245.

Supporting information

S1. Adsorption kinetics

S1.1. Pseudo-first-order model

The linear form of Lagergren pseudo-first-order rate in is given as [S1–S5]:

$$\log\left(q_e - q_t\right) = \log q_e - \frac{K_1 t}{2.303} \tag{S1}$$

where k_1 (/min), q_e and q_t denoted rate constant of pseudo-first-order model, concentration of Pb(II) adsorbed at equilibrium and time t respectively.

S1.2. Pseudo-second-order model

It is shown as [S4,S6,S7]:

$$\frac{t}{q_t} = \frac{1}{k_2 q_e^2} + \frac{t}{q_e} \tag{S2}$$

where k_2 (g/mg min) is the rate constant of pseudo-second-order model.

S1.3. Elovich model

It is represented as [S8,S9]:

$$q_t = \frac{1}{\beta}\ln\left(\alpha\beta\right) + \frac{1}{\beta}\ln t \tag{S3}$$

where α (mg/g min) and β (g/mg) are constant. The parameter α is initial adsorption rate and β is the extent of surface coverage and activation energy for chemisorption.

S1.4. Liquid-film diffusion model

It is expressed as [S10]:

$$\ln\left(1 - F\right) = -K_{\text{fd}} t \tag{S4}$$

where K_{fd} is liquid-film diffusion rate constant and $F = q_t/q$.

S1.5. Modified Freundlich equation

It was originally developed by Kuo and Lotse [S6,S11]:

$$q_t = kC_o t^{1/m} \tag{S5}$$

where k, C_0, t and m are adsorption rate constant (L/g min), initial concentration (mg/L), contact time (min) and the Kuo–Lotse constant respectively. Its linear form is shown as:

$$\ln q_t = \ln\left(kC_o\right) + \frac{1}{m}\ln t \tag{S6}$$

S1.6. Bangham equation

Bangham equation is expressed as [S4,S9]:

$$\log\log\left(\frac{C_o}{C_o - q_t m}\right) = \log\left(\frac{k_o m}{2.303V}\right) + \alpha\log t \tag{S7}$$

where m is mass of the palm leaves (adsorbent) employed (g/L), V is volume of Pb(II) aqueous solution (mL), α (<1) and k_0 (mL/(g/L) are constants.

S2. Adsorption isotherms

S2.1. Langmuir isotherm

It is based on the maximum adsorption corresponds to the saturated monolayer of liquid molecules on the solid surface. It is represented as follows [S7,S12,S13].

$$\frac{C_e}{q_e} = \frac{1}{K_L Q_m} + \frac{C_e}{Q_m} \tag{S8}$$

where K_L is Langmuir constant (L/mg) and Q_m is Langmuir monolayers adsorption capacity (mg/g), C_e is supernatant concentration at equilibrium state of the system (mg/L), and q_e is the amount of Pb(II) adsorbed at equilibrium state of system (mg/g). The essential characteristics of Langmuir isotherm can be expressed in term of dimensionless constant separation factor R_L that is given by [S14].

$$R_L = \frac{1}{1 + K_L C_o} \tag{S9}$$

The value of R_L indicated the shape of the isotherm to be either unfavorable ($R_L > 1$), linear ($R_L = 1$), favorable ($0 < R_L > 0$), or irreversible ($R_L = 0$) [S15].

S2.2. Freundlich isotherm

It is an empirical relation employed to explain the heterogeneous system. It is shown as [S16].

$$\log q_e = \log K_f + \frac{1}{n}\log C_e \tag{S10}$$

where K_f and n_F are Freundlich constant.

S2.3. Temkin isotherm

The linear form of Temkin isotherm is represented as [S17]:

$$q_e = B_T \ln A_T + B_T \ln C_e \tag{S11}$$

where $B_T = RT/b_T$, R is gas constant (8.31 J/mol K) and T is absolute temperature (K). The constant b_T is related to the heat of adsorption and A_T is equilibrium binding constant coinciding to the maximum binding energy.

S2.4. Dubinin–Radushkevich isotherm

It is expressed as [S17]:

$$\ln q_e = \ln q_m - \beta \varepsilon^2 \quad \text{(S12)}$$

where β (mol²/KJ) is constant related to the adsorption energy and ε is the Polanyi potential can be determined by using below relationship.

$$\varepsilon = RT \ln\left(1 + \frac{1}{C_e}\right) \quad \text{(S13)}$$

where R is gas constant (8.31 KJ/mol) and T is absolute temperature (K). The mean free energy E (KJ/mol) can be calculated by Eq. (S14).

$$E = \frac{1}{\sqrt{2\beta}} \quad \text{(S14)}$$

S3. Adsorption thermodynamics

The values of change in Gibb's free energy (Δ*G*°), enthalpy (Δ*H*°) and entropy (Δ*S*°) were measured by using below relationships:

$$\ln K_c = \frac{\Delta S^\circ}{R} - \frac{\Delta H^\circ}{RT} \quad \text{(S15)}$$

$$K_c = \frac{C_a}{C_e} \quad \text{(S16)}$$

$$\Delta G^o = \Delta H^o - T\Delta S^o \quad \text{(S17)}$$

where K_c, Δ*G*°, Δ*H*° and Δ*S*° are equilibrium constant, change in Gibb's free energy (kJ/mol), enthalpy (kJ/mol) and entropy (J/mol K) respectively.

S4. References

[S1] S. Zafar, M.I. Khan, M. Khraisheh, S. Shahida, T. Javed, M.L. Mirza, N. Khalid, Use of rice husk as an efective sorbent for the removal of cerium ions from aqueous solution: kinetic, equilibrium and thermodynamic studies, Desal. Water Treat., 150 (2019) 124–135.

[S2] M.I. Khan, S. Zafar, A.R. Buzdar, M.F. Azhar, W. Hassan, A. Aziz, Use of citrus sinensis leaves as a bioadsorbent for removal of congo red dye from aqueous solution, Fresenius Environ. Bull., 27 (2018) 4679–4688.

[S3] M.I. Khan, S. Zafar, M.F. Azhar, A.R. Buzdar, W. Hassan, A. Aziz, Majeda Khraisheh, Leaves powder of syzgium cumini as an adsorbent for removal of congo red dye from aqueous solution, Fresenius Environ. Bull., 27 (2018) 3342–3350.

[S4] M.I. Khan, A. Shanableh, J. Fernandez, M.H. Lashari, S. Shahida, S. Manzoor, S. Zafar, A. Rehman, N. Elboughdiri, Synthesis of DMEA-grafted anion exchange membrane for adsorptive discharge of methyl orange from wastewaters, Membranes, 11 (2021) 166.

[S5] I.W. Almanassra, V. Kochkodan, G. McKay, M.A. Atieh, T. Al-Ansari, Kinetic and thermodynamic investigations of surfactants adsorption from water by carbide-derived carbon, J. Environ. Sci. Health, Part A, 56 (2021) 1206–1220.

[S6] M.I. Khan, M.H. Lashari, M. Khraisheh, S. Shahida, S. Zafar, P. Prapamonthon, A. Rehman, S. Anjum, N. Akhtar, F. Hanif, Adsorption kinetic, equilibrium and thermodynamic studies of Eosin-B onto anion exchange membrane, Desal. Water Treat., 155 (2019) 84–93.

[S7] I.W. Almanassra, V. Kochkodan, G. Ponnusamy, G. McKay, M. Ali Atieh, T. Al-Ansari, Carbide derived carbon (CDC) as novel adsorbent for ibuprofen removal from synthetic water and treated sewage effluent, J. Environ. Health Sci. Eng., 18 (2020) 1375–1390.

[S8] M.A. Khan, M.I. Khan, S. Zafar, Removal of different anionic dyes from aqueous solution by anion exchange membrane, Membr. Water Treat., 8 (2017) 259–277.

[S9] M.I. Khan, S. Akhtar, S. Zafar, A. Shaheen, M.A. Khan, R. Luque, A. Rehman, Removal of Congo Red from aqueous solution by anion exchange membrane (EBTAC): adsorption kinetics and thermodynamics, Materials, 8 (2015) 4147–4161.

[S10] L. Liu, Y. Lin, Y. Liu, H. Zhu, Q. He, Removal of methylene blue from aqueous solutions by sewage sludge based granular activated carbon: adsorption equilibrium, kinetics, and thermodynamics, J. Chem. Eng. Data, 58 (2013) 2248–2253.

[S11] M.I. Khan, J. Su, L. Guo, Development of triethanolamine functionalized-anion exchange membrane for adsorptive removal of methyl orange from aqueous solution, Desal. Water Treat., 209 (2021) 342–352.

[S12] I. Langmuir, The constitution and fundamental properties of solids and liquids, J. Franklin Inst., 183 (1917) 102–105.

[S13] I.W. Almanassra, G. McKay, V. Kochkodan, M. Ali Atieh, T. Al-Ansari, A state of the art review on phosphate removal from water by biochars, Chem. Eng. J., 409 (2021) 128211.

[S14] T.W. Weber, R.K. Chakravorti, Pore and solid diffusion models for fixed-bed adsorbers, AIChE J., 20 (1974) 228–238.

[S15] G. McKay, Adsorption of dyestuffs from aqueous solutions with activated carbon I: Equilibrium and batch contact-time studies, J. Chem. Technol. Biotechnol., 32 (1982) 759–772.

[S16] H. Freundlich, Uber die adsorption in lasugen (Leipzig), Z. Phys. Chem., A, 57 (1906) 385–470.

[S17] M.I. Khan, S. Zafar, M.A. Khan, F. Mumtaz, P. Prapamonthon, A.R. Buzdar, Bougainvillea glabra leaves for adsorption of congo red from wastewater, Fresenius Environ. Bull., 27 (2018) 1456–1465.